

Deep Learning Framework with Uncertainty Quantification for Survey Data: Assessing and Predicting Diabetes Mellitus Risk in the American Population

Marcos Matabuena*¹, Juan C. Vidal², Rahul Ghosal³, and Jukka-Pekka Onnela¹

¹Department of Biostatistics, Harvard University

²Universidad de Santiago de Compostela

³Department of Epidemiology and Biostatistics, University of South Carolina

April 1, 2024

Abstract

Complex survey designs are commonly employed in many medical cohorts. In such scenarios, developing case-specific predictive risk score models that reflect the unique characteristics of the study design is essential. This approach is key to minimizing potential selective biases in results. The objectives of this paper are: (i) To propose a general predictive framework for regression and classification using neural network (NN) modeling, which incorporates survey weights into the estimation process; (ii) To introduce an uncertainty quantification algorithm for model prediction, tailored for data from complex survey designs; (iii) To apply this method in developing robust risk score models to assess the risk of Diabetes Mellitus in the US population, utilizing data from the NHANES 2011-2014 cohort. The theoretical properties of our estimators are designed to ensure minimal bias and the statistical consistency, thereby ensuring that our models yield reliable predictions and contribute novel scientific insights in diabetes research. While focused on diabetes, this NN predictive framework is adaptable to create clinical models for a diverse range of diseases and medical cohorts. The software and the data used in this paper is publicly available on GitHub.

Keywords: Survey data; neural networks; uncertainty quantification; conformal prediction; NHANES data

1 Introduction

Although not a primary focus among data practitioners, experimental design is critically important in addressing the current biomedical reproducibility crisis [5, 1, 28]. Its significance, underscored by Ronald Fisher’s pioneering work, is evident in the evolution of modern statistics [36]. In medical research, experimental design is essential in shaping studies that support the development and validation of new drugs and clinical treatments, especially in randomized

*Corresponding author. Email: mmatabuena@hsph.harvard.edu

clinical trials [30]. Beyond these trials, the sampling methods in national-representative studies like NHANES (National Health and Nutrition Examination Survey) profoundly affect the generalizability of clinical risk score models [24, 25].

NHANES exemplifies a well-designed study, renowned for its reliability and comprehensive data collection, monitoring disease prevalence and health habits in the U.S. Unlike other clinical studies, such as the UK Biobank, where individuals voluntarily participate, and the selection bias is prevalent [31, 6], NHANES employs a multi-stage complex design, drawing from a random sample of the U.S. This approach includes different hierarchical levels, like states and cities, and incorporates post-stratification techniques to minimize non-responder impact, enhance representativeness, and improve the efficiency of estimators.

This intricate procedure ensures accurate conclusions, and enhance monitoring changes over time through various metabolic and physiological tests conducted in different periods. NHANES is a benchmark study, but the success of statistical analysis relies heavily on adopting methods that accommodate its experimental design.

In biomedical research, developing risk assessment scores is vital for healthcare planning, particularly in public health [23, 17, 34]. These scores, which estimate the likelihood of contracting specific diseases, are crucial for identifying at-risk individuals [10]. Based on these assessments, healthcare strategies like tailored follow-ups, regular check-ups, and non-invasive interventions can be implemented, reducing health costs and improving population health [13, 32, 29].

However, constructing disease-specific risk scores using observational data is prone to selection bias [6], challenging the generalizability of results. This issue is evident in diabetes research [26], where the predictive capacity of risk scores varies, and is influenced by different population genetics, demographics, and experimental design quality. Practical challenges, such as costs and technical limitations, often hinder random sampling.

To overcome these challenges, researchers frequently use multi-stage survey designs, as seen in NHANES. This approach involves conducting studies at various levels, targeting different subpopulations. Despite its prevalence, the integration of specific survey designs with machine learning models and survey weight estimations remains limited. Additionally, the inferential statistics for such models face inherent problems.

To bridge this gap and potentially impact clinical conclusions in biomedical studies (see to Table 1 for NHANES case), we propose a novel neural network framework for prediction in this context, incorporating uncertainty quantification based on conformal prediction techniques. We apply these methods to develop reliable risk scores for detecting Diabetes Mellitus in the US population.

Aspect	Impact of Not Using Correct NHANES Survey Weights
Bias in Estimates	Biased statistical results, misrepresenting certain groups
Loss of Representativeness	Results not reflective of U.S. civilian non-institutionalized population
Policy Decisions	Potential misinformed public health policies and resource allocation
Statistical Inaccuracy	Incorrect standard errors, confidence intervals, and p-values
Ethical Considerations	Ethical concerns due to disproportionate exclusion of minority groups

Table 1: Impacts of Not Using Survey Weights in NHANES Data Analysis

1.1 Diabetes Study Case

Diabetes Mellitus represents a significant public health challenge, currently affecting approximately 12% of the U.S. population. A notable concern, particularly in Type 2 Diabetes, is the high rate of undiagnosed cases. The CDC in 2020 reported that around 21% of diabetes cases in the U.S. remained undetected [9]. Our recent research suggests that this percentage could be even higher [16].

The prevalence of sedentary lifestyles, especially in developed countries, contributes to a worrying projected increase in diabetes cases. Currently affecting about 9.3% of the global population, projections suggest an increase to 10.2% by 2030 and 10.9% by 2045. This rising trend underscores the urgent need for effective public health strategies.

The economic impact of diabetes is substantial, with the total cost in the U.S. estimated at \$412.9 billion, including \$306.6 billion in direct medical expenses and \$106.3 billion in indirect costs [29]. The burden of diabetes extends beyond financial costs, significantly affecting life expectancy and quality of life, primarily due to late diagnoses and poor glycemic control. These issues often lead to severe complications, including cardiovascular problems.

There is an increasing need to develop new precision medicine strategies based on a data-driven approach. These strategies can involve the development of new screening methods and the prescription of treatments with dynamic information obtained from wearable and electronic record devices.

In the case of Diabetes Mellitus, the diagnosis typically involves biomarkers such as glycosylated hemoglobin (A1C) and fasting plasma glucose (FPG). While FPG tests are cost-effective, A1C testing, a primary biomarker for diabetes, is more expensive and complex. Despite its widespread use, particularly in non-risk groups, A1C testing presents significant challenges. Medical guidelines, including those from the American Diabetes Association (ADA), recommend using both A1C and FPG, along with oral glucose tolerance tests, especially in cases of gestational diabetes, for a comprehensive assessment.

In the area of disease diagnosis and screening, statistical and machine learning models, leveraging clinical variables, show promise as a tool in the identification of high-risk individuals. These predictive models can stratify patients effectively, allowing for personalized clinical approaches in line with precision medicine. However, their predictive power can vary across different patient demographics and in real-world applications with limited sample sizes, which poses challenges in accurately determining patients' glucose status.

In this paper, we address these challenges by utilizing data from the National Health and Nutrition Examination Survey (NHANES) 2011-2014. Given the complexity of the survey design and the relative scarcity of non-parametric models in this domain, we introduce novel neural network estimators. These estimators are designed to ensure universal approximation capabilities in predictive tasks. Furthermore, we developed a new uncertainty quantification framework based on conformal inference techniques for survey data, enhancing our ability to quantify the predictive limits of these models. This holistic approach aims to improve the precision and applicability of predictive models for Diabetes Mellitus.

1.2 Neural Network Models and machine learning models for Survey Data

The application of non-parametric regression models in survey data analysis is a relatively unexplored area, as indicated in [21]. Traditional methods, such as the Nadaraya-Watson estimator [15] and local polynomial regression, were proposed but are very sensitive to a large

number of predictors. Recently, machine learning algorithms, such as neural networks and random forests, have been recommended in the literature as non-parametric alternatives to classical regression algorithms. Nevertheless, their generalization to inferential and predictive tasks in the field of complex survey design, such as survey data, has not been proposed. To the best of our knowledge, the closest proposal was the kernel ridge regression models proposed by [25] for functional and distributional data analysis applications.

The goal of this paper is to overcome this gap in the literature and propose a general neural network (NN) framework for classification and regression models, pointwise predictions, and uncertainty quantification for survey data.

Given the common prevalence of nonlinear biological data, the universal properties of neural networks are promising, together with their robustness in comparison with other estimators in high-dimensional settings, as a potential alternative. From the perspective of biomedical applications, the novel NN predictive framework provides the scientific community the opportunity to develop new, general disease risk scores that are trustworthy due to the incorporation of uncertainty quantification into model output predictions.

Summary of Contributions

The contributions of this article are summarized below:

- **Neural Network Models for Survey Data:** Our paper introduces a novel application of specific neural network models as estimators for complex survey data, focusing on developing risk scores within cohorts like NHANES.
- **Prediction Uncertainty Quantification:** We propose a method for quantifying prediction uncertainty through the use of conformal inference techniques, specifically adapted to meet the challenges inherent in complex survey data. Although the assumptions of exchangeability are violated, and non-asymptotic guarantees cannot be upheld, the algorithms remain consistent.
- **Versatile Framework:** Our framework operates in both regression and classification settings. In regression, we focus on conditional mean estimation, while in classification, we explore quantile regression to develop a survey conformal prediction algorithm. This approach addresses a gap in the literature concerning quantile regression and non-linear regression algorithms with survey data (see [12]).
- **Diabetes Application Analysis:** We explore models of varying complexity and economic cost in the context of diabetes. Our analysis compares performance in detecting Diabetes Mellitus across subpopulations, providing a nuanced trade-off analysis between prediction capacity and economic cost. We advocate for an economically feasible model with enhanced detection accuracy for specific patient groups.
- **Patient Phenotype Identification:** We apply the novel uncertainty predictive framework for survey data to identify patient phenotypes associated with high prediction uncertainty, providing interpretable rules for to stratify the patients according the expected model uncertainty.

Outline of the Paper

The structure of the paper is organized as follows: Section 2 introduces our novel neural network models specifically designed for survey data, along with the proposed approach to quantify uncertainty in this context. In Section 3, we present a simulation study within a binary classification framework. This section validates our models and examines their empirical performance, particularly focusing on neural network classification and uncertainty quantification. Section 4 details a diabetes case study, applying the algorithms discussed in Section 2 and analyzing the results obtained. Section 5 discusses the methodological contributions of our study, the broader applicability of our models in the field of biomedical science, and the implications of our findings utilizing the NHANES dataset. This section also addresses the limitations of our scientific diabetes application and suggests potential directions for future research.

2 Methodology

2.1 Model estimation: Survey Neural networks models

Suppose we observe a random sample $\mathcal{D}_n = \{(X_i, Y_i) \sim P\}_{i=1}^n$ drawn from a finite population \mathcal{M} of size n , according to a specific survey design. For each unit i ($i = 1, \dots, n$), we associate a weight w_i that indicates the number of population units represented by the i -th sample unit. In this paper, we assume that $w_i = 1/\pi_i$, where π_i is the probability of selecting the i -th unit under some probability sampling design. For the final weight derivation w_i , in our scientific applications, we consider specific post-stratification corrections that compensate for non-responders in the NHANES design (see specific details about NHANES design ¹).

Without loss of generality, we assume that each predictor $X_i \in \mathbb{R}^p$, and the response variable $Y_i \in \{1, \dots, K\}$ denote the set of K different categories in a multi-class classification problem or, in another case, the response is a continuous-scalar biomarker in the case of regression modeling, such that each $Y_i \in \mathbb{R}$. For practical purposes of new predictive regression algorithms, we only need to modify the specific loss functions ℓ to fit a model or other.

Deep neural networks [11] (DNNs) use the composition of a series of the simple nonlinear functions to model nonlinearity. Specifically, we can write,

$$h^{(L)} = g^{(L)} \circ g^{(L-1)} \circ \dots \circ g^{(1)},$$

where \circ denotes the composition of two functions, L is the number of hidden layers (or depth) of the neural network, and $h^{(0)} = x$. We can recursively define $h^{(l)} = g^{(l)}(h^{(l-1)})$ for all $l = 1, 2, \dots, L$. Feed-forward neural networks are a specific type of neural network that defines

$$h^{(l)} = g^{(l)}(h^{(l-1)}) = \sigma(\omega^{(l)}h^{(l-1)} + b^{(l)}), \quad (1)$$

where $\omega^{(l)}$ and $b^{(l)}$ are the weight matrix and the intercept, respectively, associated with the l -th layer, for $l = 1, \dots, L$. Here, $\sigma(\cdot)$ is an activation function applied element-wise. In this paper, we use the popular ReLU function, given by

$$\sigma(z_j) = \max(z_j, 0), \quad (2)$$

where j -coordinate of the vector z .

¹(<https://www.cdc.gov/nchs/nhanes/tutorials/weighting.aspx>)

Given an output from the final hidden layer $h^{(L)}$ and a label y , we aim to minimize a loss function to obtain the model parameters. In this paper, we adopt the weighted cross-entropy loss function, incorporating survey weights into the estimation process. The set of parameter θ are obtained solved the following optimization problem:

$$\hat{\theta} = \arg \min_{\theta} \sum_{i=1}^n w_i \cdot \ell(Y_i, \log f(X_i; \theta)) = \arg \min_{\theta} \sum_{i=1}^n \sum_{k=1}^K \mathbb{I}\{Y_i = k\} \cdot w_i \cdot \log f_k(X_i; \theta), \quad (3)$$

where $\theta = \{\omega^{(l)}, b^{(l)} \mid 1 \leq l \leq L + 1\}$ represents the set of model parameters, including the weights $\omega^{(l)}$ and biases $b^{(l)}$ for each layer l up to layer $L + 1$. Here, w_i denotes the survey weight for observation i , $\ell(\cdot, \cdot)$ is the loss function comparing the predicted and actual values, and

$$f_k(x; \theta) = \frac{\exp(z_k)}{\sum_{j=1}^K \exp(z_j)}, \quad \forall k \in \{1, \dots, K\}, \quad \text{where } z = \sigma(\omega^{(L+1)}h^{(L)} + b^{(L+1)}) \in \mathbb{R}^K. \quad (4)$$

In the literature on survey data analysis, practitioners often use weighting-type estimators to obtain reliable estimates. A common strategy involves integrating loss functions with the Horvitz-Thompson estimator. This method assigns weights to sampled units based on their probability of selection. This approach is frequently utilized to efficiently obtain estimators that minimize variance and ensure unbiased characteristics. Similarly, the use of representative weights guarantees statistical consistency.

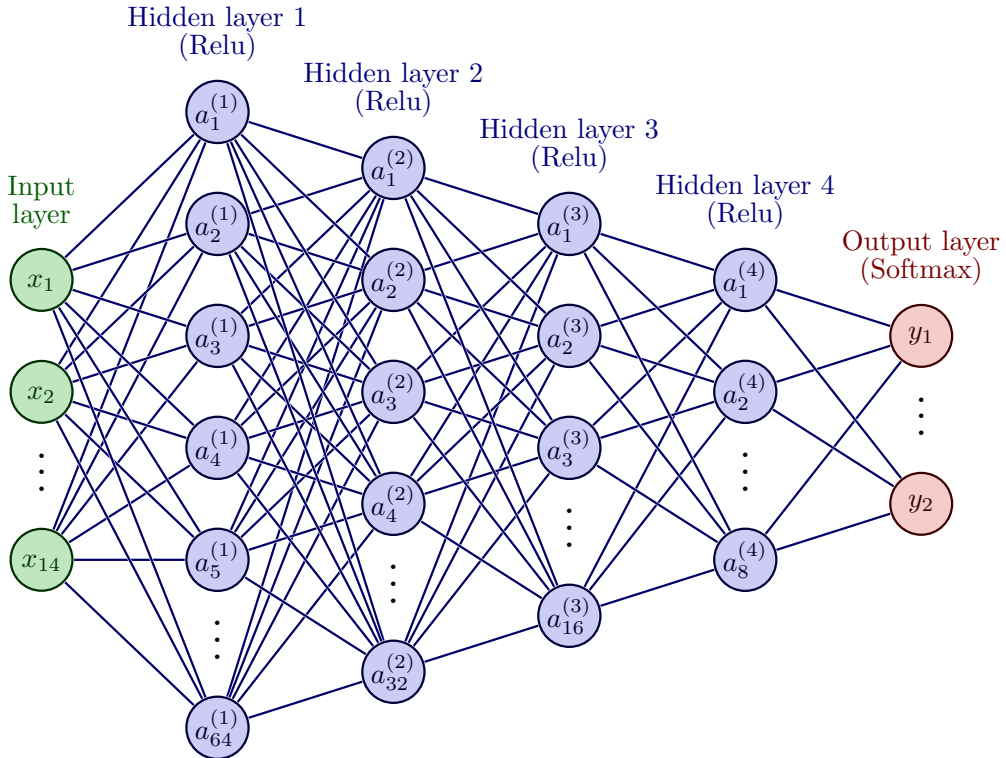


Figure 1: Neural network architecture considered in this paper.

2.2 Computational details of NN

In our scientific application, we focus on a binary classification problem, distinguishing between two classes: i) diabetes and ii) non-diabetes. Our approach utilizes a neural network architecture with a depth of L and two layers at each level. An abstract representation of the neural network architecture can be found in Figure 4. To fine-tune the model and select the optimal architecture, we partition the dataset \mathcal{D}_n into three disjoint subsets: training ($\mathcal{D}_{\text{train}}$), architecture selection ($\mathcal{D}_{\text{architecture}}$), and testing ($\mathcal{D}_{\text{test}}$), with proportions of 50%, 30%, and 20% respectively. We adopt a cross-validation strategy, repeating the model evaluation process 10 times to ensure robust validation of the model’s performance across various metrics.

For each subject i , we denote the algorithm’s predicted label as \hat{Y}_i and the estimated probability of having diabetes as $\hat{p}_i = \mathbb{P}(Y_i = 1 \mid X = X_i)$. We define D as the set of indices for diabetes patients and ND for non-diabetes patients. The performance metrics considered are detailed in Table 2.

To optimize the model parameters, we employ stochastic gradient descent (SGD) with the Adam algorithm, leveraging its adaptive learning rate properties. This optimization is facilitated by the auto-differentiable capabilities of PyTorch computational framework.

Table 2: Performance Metrics for Binary Classification with Survey Weights

Metric	Formula	Description
AUC	$\sum_{i \in D} \sum_{j \in ND} w_i w_j \left(\frac{1}{\sum_{i \in D} \sum_{j \in ND} w_i w_j} \right) k(\hat{p}_i, \hat{p}_j)$	Weighted classification performance measure
ACC	$\frac{TP+TN}{TP+TN+FP+FN}$	Proportion of correctly classified instances
REC	$\frac{TP}{TP+FN}$	Sensitivity or true positive rate
PREC	$\frac{TP}{TP+FP}$	Precision or positive predictive value
F_1	$\frac{2 \cdot \text{PREC} \cdot \text{REC}}{\text{PREC} + \text{REC}}$	Harmonic mean of precision and recall
Cross-Entropy	$-\sum_i w_i [y_i \log(\hat{p}_i) + (1 - y_i) \log(1 - \hat{p}_i)]$	Weighted log loss between predicted and actual labels

2.3 Uncertainty quantification for suvey data based on conformal prediction

2.3.1 Background about conformal prediction and uncertainty quantification

In medical studies, considerable uncertainty exists in various predictive tasks due to the large variability among individual patients [13, 3]. Although this uncertainty is often perceived negatively, it can be beneficial in different clinical situations to support decision-making [13]. Firstly, it aids in understanding the limitations of clinical prediction models. Secondly, significant uncertainty regarding patient outcomes can lead to the development of new pharmacological treatments or intervention strategies, offering novel therapeutic avenues. Thirdly, uncertainty can guide healthcare planning; for patients with unpredictable clinical courses, more frequent routine check-ups can be scheduled. Lastly, quantifying individual patient uncertainty is crucial for identifying atypical behaviors and supports the estimation of healthcare resource needs. Each of these aspects underscores the importance of incorporating uncertainty quantification into practice.

Here, let $(X_1, Y_1), \dots, (X_n, Y_n)$ be a random sample that is at least exchangeable. We focus on extending this framework to propose a new algorithm for deriving uncertainty measures based on conformal prediction. We now provide the basic foundations for regression models with a scalar response.

Consider the sequence $\mathcal{D}_n = \{(X_i, Y_i)\}_{i=1}^n$ i.i.d. random variables. Given a new i.i.d random pair (X_{n+1}, Y_{n+1}) with respect to \mathcal{D}_n , conformal prediction, as outlined by [33], provides a comprehensive family of algorithms for constructing prediction intervals independently of the regression algorithm used.

Let us consider a regression algorithm

$$\mathcal{A} : \bigcup_{n \geq 0} (\mathcal{X} \times \mathbb{R})^n \rightarrow \{\text{measurable functions } \tilde{m} : \mathcal{X} \rightarrow \mathbb{R}\},$$

which maps a data set containing any number of pairs (X_i, Y_i) , to a fitted regression function \tilde{m} . The algorithm \mathcal{A} is required to treat data points symmetrically, i.e.,

$$\mathcal{A}((x_{\pi(1)}, y_{\pi(1)}), \dots, (x_{\pi(n)}, y_{\pi(n)})) = \mathcal{A}((x_1, y_1), \dots, (x_n, y_n)) \quad (5)$$

for all $n \geq 1$, all permutations π on $[n] = \{1, \dots, n\}$, and all $\{(x_i, y_i)\}_{i=1}^n$. Next, for each $y \in \mathbb{R}$, let

$$\tilde{m}^y = \mathcal{A}((X_1, Y_1), \dots, (X_n, Y_n), (X, y))$$

denote the trained model, fitted to the training data together with a hypothesized test point (X_{n+1}, y) , and let

$$R_i^y = \begin{cases} |Y_i - \tilde{m}^y(X_i)|, & i = 1, \dots, n, \\ |y - \tilde{m}^y(X_{n+1})|, & i = n + 1. \end{cases} \quad (6)$$

The prediction interval for X is then defined as

$$\tilde{C}^\alpha(X; \mathcal{D}_n) = \left\{ y \in \mathbb{R} : R_{n+1}^y \leq \text{quant}_{1-\alpha} \left(\sum_{i=1}^{n+1} \frac{1}{n+1} \cdot \delta_{R_i^y} \right) \right\}, \quad (7)$$

where $\text{quant}_{1-\alpha} \left(\sum_{i=1}^{n+1} \frac{1}{n+1} \cdot \delta_{R_i^y} \right)$ denotes the quantile operator of order $1 - \alpha$ applied to the empirical distribution $\sum_{i=1}^{n+1} \frac{1}{n+1} \cdot \delta_{R_i^y}$.

The full conformal method is known to guarantee distribution-free predictive coverage at the target level $1 - \alpha$:

Theorem 1 (Full conformal prediction [33]). *If the data points $(X_1, Y_1), \dots, (X_n, Y_n), (X, Y)$ are i.i.d. (or more generally, exchangeable), and the algorithm treats the input data points symmetrically as in (5), then the full conformal prediction set defined in (7) satisfies*

$$\mathbb{P}(Y_{n+1} \in \tilde{C}^\alpha(X_{n+1}; \mathcal{D}_n)) \geq 1 - \alpha.$$

The same result holds true for split conformal methods, which involve estimating the regression function on $\mathcal{D}_{\text{train}}$ and the quantile on $\mathcal{D}_{\text{test}}$.

Conformal inference (both split and full) was initially proposed in terms of “nonconformity scores” $\hat{S}(X_i, Y_i)$, where \hat{S} is a fitted function that measure the extent to which a data point (X_i, Y_i) is unusual relative to a training data set $\mathcal{D}_{\text{train}}$. For simplicity, so far we have only presented the most commonly used nonconformity score, which is the residual from the fitted model

$$\hat{S}(X_i, Y_i) := |Y_i - \tilde{m}(X_i)|, \quad (8)$$

where \tilde{m} is pre-trained regression function estimated for example with the random elements of $\mathcal{D}_{\text{train}}$.

2.3.2 NHANES Study Design

The National Health and Nutrition Examination Survey (NHANES) employs a sophisticated multi-stage probabilistic sampling design to accurately reflect the U.S. civilian non-institutionalized population. This methodological framework is crucial for ensuring the representation of diverse demographic characteristics in the dataset, which is essential for epidemiological and nutritional surveillance.

The selection process begins with Primary Sampling Units (PSUs), typically comprising counties or groups of contiguous counties, chosen through probability proportional to size methods. This approach guarantees a geographically representative sample of the U.S. population. The PSUs are then subdivided into smaller segments, enabling targeted sampling within specific locales. Households within these segments are systematically sampled, and individuals are selected based on demographic criteria such as age, sex, and race/ethnicity. This stratification allows for analyses across various population groups.

However, the inherent heterogeneity across states, including variations in ethnic composition, socioeconomic status, and health outcomes, challenges the assumption of exchangeability data within NHANES. Such variability necessitates careful statistical considerations, especially when applying conformal inference algorithms that rely on the principles of exchangeability and i.i.d. assumptions for providing non-asymptotic guarantees.

2.3.3 Conformal Prediction, Concept Drift, and Survey Data algorithm

Due to the discussion of NHANES experimental design, we focus on settings in which the data $(X_i, Y_i), i = 1, \dots, n + 1$ are no longer exchangeable. Our primary focus will be on a setting in which we observe data according to

$$\begin{aligned} (X_i, Y_i) &\stackrel{\text{i.i.d.}}{\sim} P = P_X \times P_{Y|X}, i = 1, \dots, n, \\ (X_{n+1}, Y_{n+1}) &\sim \tilde{P} = \tilde{P}_X \times P_{Y|X}, \text{independently.} \end{aligned} \quad (5)$$

Notice that the conditional distribution of $Y|X$ is assumed to be the same for both the training and test data. Such a setting is often referred to as covariate shift. Then, if we know the ratio of test to training covariate likelihoods, $\frac{d\tilde{P}_X}{dP_X}$, we can still perform a modified version of conformal inference, using a quantile of a suitably weighted empirical distribution of nonconformity scores.

In the covariate shift case, where the covariate distributions P_X and \tilde{P}_X in our training and test sets differ, we now weight each nonconformity score $V_i^{(x,y)}$ (measuring how well $Z_i = (X_i, Y_i)$ conforms to the other points) by a probability proportional to the likelihood ratio $w(X_i) = \frac{d\tilde{P}_X(X_i)}{dP_X(X_i)}$. Therefore, we will no longer be interested in the empirical distribution $\frac{1}{n+1} \sum_{i=1}^n \delta_{V_i^{(x,y)}} + \frac{1}{n+1} \delta_\infty$, as in Theorem 1, but rather, in a weighted version

$$\sum_{i=1}^n p_i^w(x) \delta_{V_i^{(x,y)}} + p_{n+1}^w(x) \delta_\infty$$

where the weights are defined by

$$p_i^w(x) = \frac{w(X_i)}{\sum_{j=1}^n w(X_j) + w(x)}, i = 1, \dots, n, \quad \text{and} \quad p_{n+1}^w(x) = \frac{w(x)}{\sum_{j=1}^n w(X_j) + w(x)}. \quad (6)$$

Theorem 2. *Assume data from the model (5). Assume \tilde{P}_X is absolutely continuous with respect*

to P_X , and denote $w = \frac{d\tilde{P}_X}{dP_X}$. For any score function \mathcal{S} , and any $\alpha \in (0, 1)$, define for $x \in \mathbb{R}^d$,

$$\widehat{C}_n(x) = \left\{ y \in \mathbb{R} : V_{n+1}^{(x,y)} \leq \text{Quantile} \left(1 - \alpha; \sum_{i=1}^n p_i^w(x) \delta_{V_i^{(x,y)}} + p_{n+1}^w(x) \delta_\infty \right) \right\}. \quad (7)$$

where $V_i^{(x,y)}$, $i = 1, \dots, n+1$ are as defined in (3), and p_i^w , $i = 1, \dots, n+1$ are as defined in (6). Then \widehat{C}_n satisfies

$$\mathbb{P} \left\{ Y_{n+1} \in \widehat{C}_n(X_{n+1}) \right\} \geq 1 - \alpha.$$

For classification purposes, we focus on adapting the quantile classification algorithm [8] based on concept drift conformal principles. Algorithm 2.3.3 contains the core steps of the algorithm, that, unlike the first conformal algorithm, we propose an algorithm where the non-conformity score is based on quantile regression of the cross-entropy.

Split Survey Conformalized Quantile Classification (CQC) Input: Sample $\{(X_i, Y_i)\}_{i=1}^n$, index sets $\mathcal{I}_1, \mathcal{I}_2, \mathcal{I}_3 \subset \{1, \dots, n\}$, fitting algorithm \mathcal{A} , quantile function \mathcal{Q} , and desired confidence level α .

1. Estimate the score value \widehat{s}_i as $\widehat{s}_i = \sum_{k=1}^K 1\{Y_i = k\} w_i \log f_k(X_i; \theta)$, for $i \in \mathcal{I}_1$.
2. Fit the quantile function via

$$\widehat{q}_\alpha \in \arg \min_{q \in \mathcal{Q}} \left\{ \frac{1}{|\mathcal{I}_2|} \sum_{i \in \mathcal{I}_2} w_i \rho_\alpha(\widehat{s}_i - q(X_i)) \right\}, \quad (9)$$

where $\rho_\alpha = (1 - \alpha)[-t] + \alpha[t]$.

3. Calibrate by computing non-conformity scores $S_i = \widehat{q}_\alpha(X_i) - \widehat{s}_i$, and define

$$Q_{1-\alpha}(S, \mathcal{I}_3) := \left[1 + \frac{1}{n_3} \right] (1-\alpha) \text{ empirical quantile of } \{S_i\}_{i \in \mathcal{I}_3} \text{ using the survey weights.} \quad (10)$$

and return the predictive region function

$$\widehat{C}_{n,1-\alpha}(x) := \{k \in \{1, \dots, K\} | \widehat{s}(x, k) \geq \widehat{q}_\alpha(x) - Q_{1-\alpha}(S, \mathcal{I}_3)\}. \quad (11)$$

2.3.4 Conformal Prediction Beyond Exchangeability

In a recent paper, a more general conformal approach was proposed [4] for data that are not exchangeable. We introduce the key ideas to illustrate their application in our NHANES survey settings.

The *coverage gap* is a crucial concept in our analysis, representing the discrepancy in coverage due to non-exchangeability. It is defined as:

$$\text{Coverage gap} = (1 - \alpha) - \mathbb{P} \left\{ Y_{n+1} \in \widehat{C}_n(X_{n+1}) \right\},$$

since, under exchangeability, the method guarantees coverage with probability $1 - \alpha$. To provide an informal preview of our results, we use $Z_i = (X_i, Y_i)$ to denote the i th data point and

$$Z = (Z_1, \dots, Z_{n+1})$$

to denote the full (training and test) data sequence. Let Z^i denote this sequence after swapping the test point (X_{n+1}, Y_{n+1}) with the i th training point (X_i, Y_i) :

$$Z^i = (Z_1, \dots, Z_{i-1}, Z_{n+1}, Z_{i+1}, \dots, Z_n, Z_i).$$

To enhance robustness, our methods will incorporate weights: let $w_i \in [0, 1]$ denote a prespecified weight placed on data point i . We will demonstrate that the coverage gap can be bounded as

$$\text{Coverage gap} \leq \frac{\sum_{i=1}^n w_i \cdot d_{\text{TV}}(Z, Z^i)}{1 + \sum_{i=1}^n w_i},$$

where d_{TV} denotes the total variation distance between distributions.

In practice, the discrepancy of the coverage gap, when introducing survey weights, depends on the total variation distance $d_{\text{TV}}(Z, Z^i)$. Since survey weights are fixed, this discrepancy ultimately depends on the variance within the partial sample regarding the exchangeability hypothesis. In our case study of NHANES, we perform empirical validation to assess the extent of our algorithm's coverage gap. If the algorithm for uncertainty quantification exhibits asymptotic consistency, then as n grows, the discrepancies diminish.

:

2.4 Asymptotic NN results

According to [14], we introduce the empirical process framework, that we exploit the properties of NN for survey data.

Let $U_N \equiv \{1, \dots, N\}$, and $\mathcal{S}_N \equiv \{\{s_1, \dots, s_n\} : n \leq N, s_i \in U_N, s_i \neq s_j, \forall i \neq j\}$ be the collection of subsets of U_N . We adopt the super-population framework. Let $\{(Y_i, Z_i) \in \mathcal{Y} \times \mathcal{Z}\}_{i=1}^N$ be i.i.d. super-population samples defined on a probability space $(\mathcal{X}, \mathcal{A}, \mathbb{P}_{(Y,Z)})$, where $Y^{(N)} \equiv (Y_1, \dots, Y_N)$ is the vector of interest, and $Z^{(N)} \equiv (Z_1, \dots, Z_N)$ is an auxiliary vector. A sampling design is a function $\mathbf{p} : \mathcal{S}_N \times \mathcal{Z}^{\otimes N} \rightarrow [0, 1]$ such that

- (1) for all $s \in \mathcal{S}_N$, $z^{(N)} \mapsto \mathbf{p}(s, z^{(N)})$ is measurable,
- (2) for all $z^{(N)} \in \mathcal{Z}^{\otimes N}$, $s \mapsto \mathbf{p}(s, z^{(N)})$ is a probability measure.

The probability space we work with that includes both the super-population and the design-space is the same product space $(\mathcal{S}_N \times \mathcal{X}, \sigma(\mathcal{S}_N) \times \mathcal{A}, \mathbb{P})$. We include the construction here for convenience of the reader: the probability measure \mathbb{P} is uniquely defined through its restriction on all rectangles: for any $(s, E) \in \mathcal{S}_N \times \mathcal{A}$ (note that \mathcal{S}_N is a finite set),

$$\mathbb{P}(s \times E) \equiv \int_E \mathbf{p}(s, z^{(N)}(\omega)) d\mathbb{P}_{(Y,Z)}(\omega) \equiv \int_E \mathbb{P}_d(s, \omega) d\mathbb{P}_{(Y,Z)}(\omega) \quad (2.1)$$

We also use P to denote the marginal law of Y for notational convenience.

Given $(Y^{(N)}, Z^{(N)})$ and a sampling design \mathbf{p} , let $\{\xi_i\}_{i=1}^N \subset [0, 1]$ be random variables defined on $(\mathcal{S}_N \times \mathcal{X}, \sigma(\mathcal{S}_N) \times \mathcal{A}, \mathbb{P})$ with $\pi_i \equiv \pi_i(Z^{(N)}) \equiv \mathbb{E}[\xi_i | Z^{(N)}]$. We further assume that $\{\xi_i\}_{i=1}^N$ are independent of $Y^{(N)}$ conditionally on $Z^{(N)}$. Typically we take $\xi_i \equiv \mathbf{1}_{i \in s}$, where $s \sim \mathbf{p}$, to be the indicator of whether or not the i -th sample Y_i is observed (and in this case $\pi_i(Z^{(N)}) = \sum_{s \in \mathcal{S}_N: i \in s} \mathbf{p}(s, Z^{(N)})$), but we do not require this structure a priori. The π_i 's are often referred to as the first-order inclusion probabilities, and $\pi_{ij} \equiv \pi_{ij}(Z^{(N)}) \equiv \mathbb{E}[\xi_i \xi_j | Z^{(N)}]$ are the second-order inclusion probabilities.

We define the Horvitz-Thompson empirical measure and empirical process as follows: for $\{\pi_i\}, \{\xi_i\}, \{Y_i\}$ as above,

$$\mathbb{P}_N^\pi(f) \equiv \frac{1}{N} \sum_{i=1}^N \frac{\xi_i}{\pi_i} f(Y_i), \quad f \in \mathcal{F}$$

and the associated Horvitz-Thompson empirical process

$$\mathbb{G}_N^\pi(f) \equiv \sqrt{N} (\mathbb{P}_N^\pi - P)(f), \quad f \in \mathcal{F}$$

The name of such an empirical process goes back to [18], in which $\mathbb{P}_N^\pi(Y)$ is used as an estimator for the population mean $P(Y)$. The usual empirical measure and empirical process (i.e. with $\xi_i/\pi_i \equiv 1$ for all $i = 1, \dots, N$) will be denoted by $\mathbb{P}_N, \mathbb{G}_N$ respectively.

Assumption A. Consider the following conditions on the sampling design \mathbf{p} :

(A1) $\min_{1 \leq i \leq N} \pi_i \geq \pi_0 > 0$.

(A2 - LLN) $\frac{1}{N} \sum_{i=1}^N \left(\frac{\xi_i}{\pi_i} - 1 \right) = o_{\mathbf{P}}(1)$.

(A2-CLT) $\frac{1}{\sqrt{N}} \sum_{i=1}^N \left(\frac{\xi_i}{\pi_i} - 1 \right) = \mathcal{O}_{\mathbf{P}}(1)$.

Now, we present the key theorems [14], that are the ingredient for NN survey theory.

Theorem 3 (Glivenko-Cantelli Theorem). [14]. *Suppose that (A1) and (A2) LLN hold. If \mathcal{F} is P -Glivenko-Cantelli, then*

$$\sup_{f \in \mathcal{F}} |(\mathbb{P}_N^\pi - P)(f)| = o_{\mathbf{P}}(1).$$

Theorem 4 (Donsker Theorem). [14]. *Suppose that (A1) and (A2-CLT) hold. Further assume that:*

(D1) \mathbb{G}_N^π converges finite-dimensionally to a tight Gaussian process \mathbb{G}^π .

(D2) \mathcal{F} is P -Donsker.

Then,

$$\mathbb{G}_N^\pi \rightsquigarrow \mathbb{G}^\pi \text{ in } \ell^\infty(\mathcal{F}).$$

Theorem 5. *Consider a neural network architecture that utilizes the ReLU activation function. Let the loss function $\ell(\cdot, \cdot)$ be selected from among the weighted cross-entropy functions, the pinball loss, or the mean square error function. Under the stipulated assumptions A1-A3, which pertain to the sampling mechanism, this architecture is guaranteed to produce consistent estimates of the model parameters. Moreover, the parameters demonstrate asymptotic normality, a property attributed to the invariance principle applied to the Donsker class associated with the empirical process defined by the selected loss function.*

Proof. See Appendix. □

Theorem 6. *For a confidence level $\alpha \in (0, 1)$, the performance of the uncertainty quantification algorithm may not fulfill non-asymptotic property requirements for coverage $\mathbb{P}(Y_{n+1} \in \widehat{C}^\alpha(X_{n+1}; \mathcal{D}_n)) \geq 1 - \alpha$. However, it achieves asymptotic consistency regarding both marginal and conditional coverage. This implies that, as the sample size tends to infinity, the algorithm's coverage probability approaches the nominal level for any fixed confidence level $\alpha \in (0, 1)$,*

$$\lim_{n \rightarrow \infty} \left| (1 - \alpha) - \mathbb{P} \left(Y_{n+1} \in \widehat{C}_n(X_{n+1}, \mathcal{D}_n) \right) \right| = 0, \quad \text{in probability.}$$

Proof. See Appendix. □

3 Simulation study

We conducted a simulation study employing a two-stage cluster sampling design based on two different generative models for binary regression, where $Y \in \{0, 1\}$. In both examples, the predictor variable $X = (X_1, \dots, X_{10})^\top \in \mathbb{R}^{10} \sim \mathcal{N}_m(\mu, \Sigma)$, where $\mathcal{N}_m(\mu, \Sigma)$ denotes an m -multivariate Normal distribution with mean μ and covariance matrix Σ . For simplicity, we set $\mu = (0)_{1 \times 10}$ and $\Sigma = \mathcal{I}_{10 \times 10}$, representing a 10-dimensional vector with zeros in all entries and the identity matrix, respectively.

The conditional distribution function $Y|X \sim \text{Ber}(\pi(X))$ follows a Bernoulli distribution, where the probability parameter $\pi(X) \in [0, 1]$ is specified by different functional forms. In this paper, we consider two distinct generative models:

$$\begin{aligned} \text{a) } \pi(X) &= \frac{1}{1 + \exp(-3 + \sum_{i=1}^{10} X_i)} \\ \text{b) } \pi(X) &= \frac{1}{1 + \exp(-2 + \sum_{i=1}^3 X_i + \prod_{i=7}^{10} X_i)} \end{aligned}$$

The experimental design for the survey simulation incorporates assumptions about the hierarchical structure of clusters. In the first-stage design, clusters represent stages and regions, assuming independence of selection probabilities across stages and regions. In the second stage, clusters represent cities, and again, we assume independence of selection probabilities for each city.

Additionally, we assume a probability of selecting each state as $4/5$, and within the i -th state, there exists a variable number n_i of cities. Each city within a state is selected with equal probability, specifically $1/n_i$. The sampling mechanism and the derivation of patient probability of selection w_r are implemented using the `survey` package in **R**.

For each generative model (a) and (b), we replicate the experimental design 500 times, this is, $b = 1, \dots, B = 500$, with sample sizes varying across $N \in \{5000, 10000, 20000\}$. The performance criteria include metrics such as i) AUC; ii) Accuracy; iii) Recall; iv) Precision; v) F1 score; vi) Cross entropy. Results are presented as the *mean* \pm *sd* of the different simulations in Table 3. The consistency of results across a fixed sample size N and different performance metrics is observed. Generally, as the sample size N increases, accuracy improves, and errors decrease, leading to more stable results with reduced standard deviation. Scenario (a) exhibits lower accuracy due to less separation between the two classes, but despite utilizing a neural algorithm for modified survey design, estimators are reliable and converge to true quantities as N grows.

	Scenario a)			Scenario b)		
	$N = 5000$	$N = 10000$	$N = 20000$	$N = 5000$	$N = 10000$	$N = 20000$
AUC	0.932 \pm 0.007	0.9334 \pm 0.0054	0.93379 \pm 0.0037	0.9993 \pm 0.0036	0.999674 \pm 0.0001	0.9998 \pm 0.000764
Accuracy	0.894 \pm 0.0087	0.898 \pm 0.0055	0.900 \pm 0.003	0.9762 \pm 0.0068	0.96227 \pm 0.01137	0.96963 \pm 0.008
Recall	0.706 \pm 0.034	0.719 \pm 0.023	0.7725 \pm 0.0163	0.952 \pm 0.0150	0.96227 \pm 0.11342	0.96963 \pm 0.008
Precision	0.875 \pm 0.019	0.877 \pm 0.012	0.878 \pm 0.007	0.976 \pm 0.012	0.9859 \pm 0.0081	0.991 \pm 0.005
F1 Score	0.773 \pm 0.025	0.783 \pm 0.0015	0.7881 \pm 0.010	0.962 \pm 0.106	0.972 \pm 0.00771	0.979 \pm 0.0049
Cross-Entropy	1.262 \pm 0.0136	1.200 \pm 0.092	1.174 \pm 0.062	0.259 \pm 0.082	0.204 \pm 0.612	0.163 \pm 0.043

Table 3: Summary of Simulation Results across Scenarios (a) and (b) with Varied Sample Sizes $N \in \{5000, 10000, 20000\}$. Mean and standard deviation are reported for the following performance metrics: i) Area Under the Curve (AUC); ii) Accuracy; iii) Recall; iv) Precision; v) F1 Score; vi) Cross Entropy.

3.1 Uncertainty Quantification

In the context of conformal prediction for survey data, we leverage the generative models from the simulation scenarios (a) and (b). However, our focus shifts to evaluating model performance based on marginal coverage across different confidence levels $\alpha = 0.95, 0.9, 0.8$. Specifically, we assess the independent random sample $\mathcal{D}_{\text{test}}$, comprising $N = 5000$ data points, by quantifying the probability metrics $\mathbb{P}(Y \in \hat{C}^\alpha(X))$ across multiple simulations $b = 1, \dots, B$. The results of this simulation exercise for scenarios (a) and (b) are depicted in Figures 2 and 3, respectively.

Our findings affirm the non-asymptotic property of conformal prediction, demonstrating that $\mathbb{P}(Y \in \hat{C}^\alpha(X)) \geq \alpha$. This observation aligns with our experimental design, which conditions data as exchangeable across clusters. Notably, the boxplots illustrate a convergence toward the nominal value as the sample size N increases. Furthermore, the variability in the boxplots diminishes, indicating consistent and reliable model performance in these specific simulation examples.

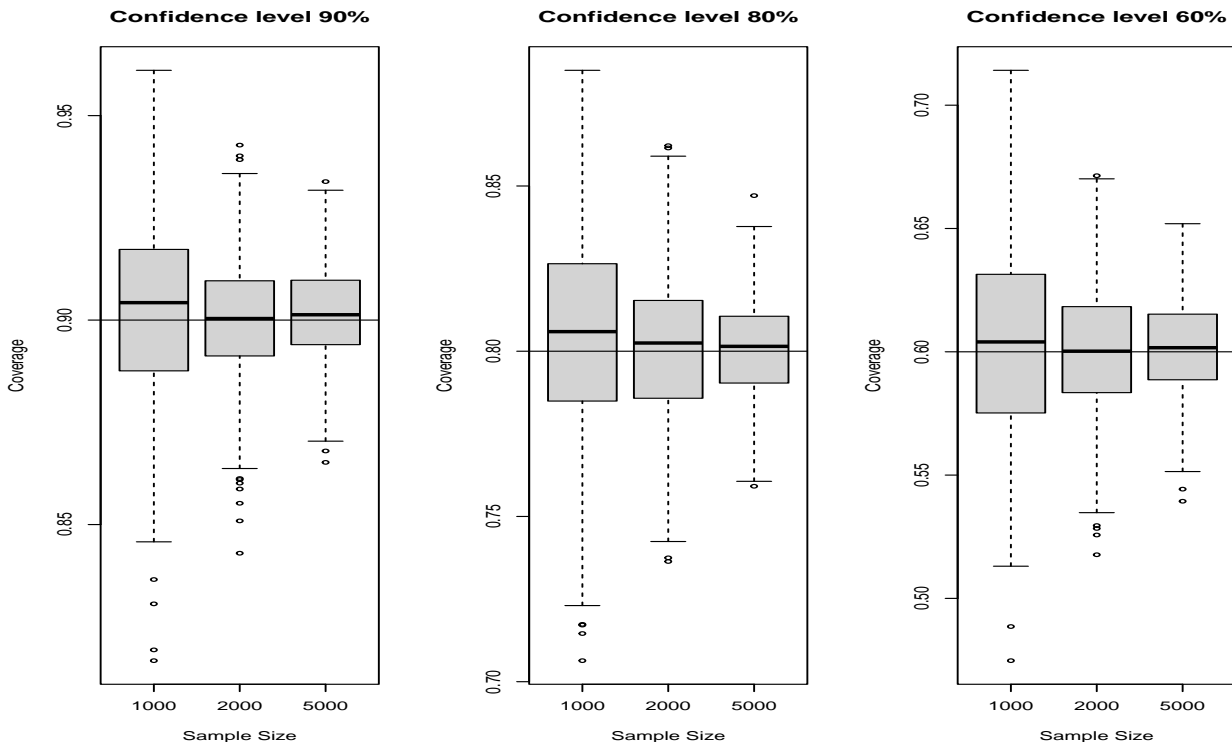


Figure 2: Results of conformal simulation exercise for the generative model a)

4 NHANES diabetes study case

4.1 Literature review: Predictive models for predictive diabetes risk models

In the pursuit of stratifying patients' risk for diabetes, various diabetes scores, such as the Finnish (FINDRISC) [22] and the German (GDRS) [27], were developed over a decade ago. These scores leverage logistic regression for predicting the probability of developing diabetes in ten years or employ survival models like Cox regression to predict the time to diabetes onset.

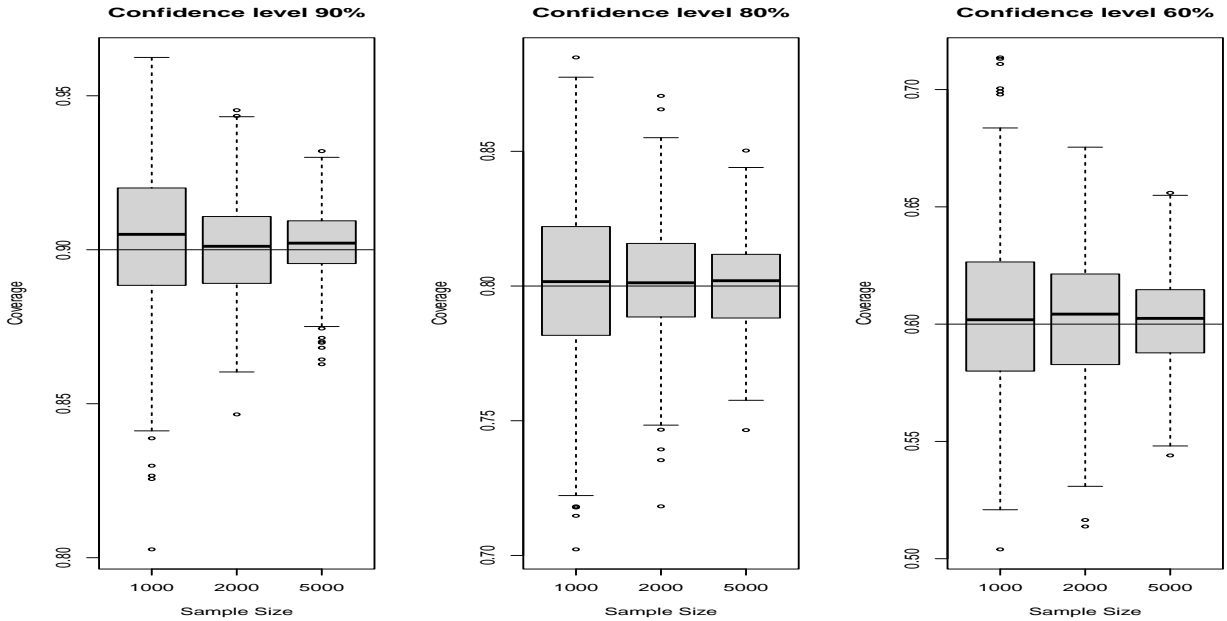


Figure 3: Results of conformal simulation exercise for the generative model b)

They incorporate easily obtainable variables such as age, sex, anthropometric measurements, lifestyle, family history, and medication.

More recently, several machine-learning methods for predicting progression to diabetes from a healthy or prediabetes state have been proposed, demonstrating promising performance [35, 7]. However, these studies, while including a large number of subjects, are based on observational data, and subjects with only partially available data are often excluded. Hence, caution is warranted when applying these results for decision-making.

Our modeling strategy diverges from previous approaches as we aim to predict whether patients have diabetes mellitus at a fixed point in time based on their current characteristics. From a statistical standpoint, this approach offers advantages, allowing for an increased number of cases and mitigating imbalance issues related to prior approximations. Additionally, unlike previous models, we introduce a survey sampling mechanism into the model, enabling us to derive reliable and generalizable conclusions about predictions for the American population.

4.2 NHANES 2011-2014 data

Our study draws upon data sourced from the National Health and Nutrition Examination Survey (NHANES) waves 2011–2014 [20]. NHANES is a comprehensive initiative aimed at furnishing a wide array of descriptive health and nutrition statistics for the civilian non-institutionalized population of the United States.

The data collection process involves both an interview and an examination. The interview captures person-level demographic, health, and nutrition information, while the examination entails physical measurements, including blood pressure, dental examinations, and the collection of blood and urine specimens for laboratory testing. Our analysis encompasses a cohort of 5011 older adults, aged 10 to 80 years.

In our investigation, we considered various factors such as age (treated as both a categorical and continuous variable), race, gender, cancer or diabetes diagnosis (categorical variables), blood pressure, combined grip strength measure, body mass index (BMI), and biochemical

biomarkers, including cholesterol and triglycerides (treated as continuous variables).

The race variable was encoded as follows: 1=Mexican American; 2=Other Hispanic; 3=Non-Hispanic white; 4=Non-Hispanic black; 5=Non-Hispanic Asian; and 6=Other Race, encompassing multi-racial categories. A comprehensive listing of the variables employed in our models is provided in Table 4.

Table 4: Clinical Characteristics of Diabetes and Non-Diabetes Patients

Variable	Diabetes (32%)	No Diabetes (68%)
Age	54.1 ± 15.2	44.8 ± 16.2
Height	88.3 ± 22.5	80.8 ± 19.3
Weight	169.1 ± 10.1	169.4 ± 9.6
BMI	30.8 ± 7.13	28.08 ± 6.16
Waist	96.9 ± 14.9	105.6 ± 16.8
Diastolic Blood Pressure	71.1 ± 12.2	70.9 ± 11.2
Systolic Blood Pressure	126.0 ± 16.5	119.2 ± 15.5
Pulse	73.7 ± 12.1	71.5 ± 11.36
Cholesterol (mmol/L)	5.0 ± 1.1	4.98 ± 1.0
Triglycerides (mmol/L)	2.09 ± 1.7	1.55 ± 1.06
Gender Male	47%	50%
Glucose (mg/dL)	123 ± 48	89 ± 10
Glycosylated Hemoglobin %	6.22 ± 1.35	5.33 ± 0.35

4.3 Diabetes Definition

In our analysis involving 5011 patients, each weighted with their respective survey weights w_i ($i = 1, \dots, N = 5011$), we define the diagnostic status of diabetes as binary, denoting "1" for the presence of diabetes and "0" for the absence of diabetes.

The diagnostic criteria for Type 2 Diabetes, as specified by the American Diabetes Association (ADA), are as follows [2]:

1. A fasting plasma glucose (FPG) level of 126 mg/dL (7.0 mmol/L) or higher, or
2. A hemoglobin A1c (HbA1c) level of 6.5% (48 mmol/mol) or higher.
3. Previously diagnosed with diabetes by a medical professional.

Utilizing this definition and the corresponding labeled outcomes, we employed a diverse set of models with varying levels of complexity in terms of economic cost and laboratory testing.

4.4 Model performance results

In our study, we meticulously evaluated seven predictive models for diabetes, focusing on a detailed comparison of their performance based on key metrics such as the area under the curve (AUC), accuracy, recall, precision, F1 score, and cross-entropy. We also considered the cost implications of deploying each model. The initial models, especially Models 1 to 4, gradually incorporated more clinical variables, starting from basic demographic information and extending to include physiological and metabolic markers like cholesterol and triglycerides. Model 4, which introduced metabolic markers into its variable set, demonstrated a significant boost in

performance with an AUC of 0.74 and an accuracy of 67%. This improvement underscored the value of including metabolic indicators in enhancing the model’s diagnostic capabilities.

Diving deeper into the specifics, Model 5 represented a substantial advancement in predictive accuracy, achieving an AUC of 0.832 and an accuracy rate of 73.9%, with precision standing at 77.4%. This model was notably enhanced by the inclusion of glycosylated hemoglobin, a critical marker for diabetes, highlighting the strategic importance of selecting relevant clinical variables to improve model efficacy.

Model 7, our most advanced configuration, showcased the highest performance levels across all evaluated metrics, with an impressive AUC of 0.92, accuracy of 81%, and precision of 78.6%. The success of Model 7 can be attributed to its comprehensive integration of a wide range of clinical variables, meticulously chosen to capture the complex nature of diabetes. The analysis of costs associated with each model revealed a clear link between a model’s complexity and its operational costs, with Model 7 standing out for its precision despite being the most costly option.

Our investigation highlights the critical role of variable selection in enhancing the predictive power of models for diabetes. The notable improvements in model performance from Models 1 through 7, particularly with the inclusion of a broader set of clinical variables in the more advanced models, advocate for a deliberate and informed approach to selecting variables. Such a strategy not only maximizes the accuracy of predictions but also underscores the need to balance the enhanced predictive capabilities against the practical considerations of cost and implementation in a clinical setting. The outcomes of this study encourage a thoughtful approach to developing predictive models for diabetes, prioritizing the careful selection of variables to achieve the best balance between accuracy, cost-effectiveness, and clinical utility.

Variable	Model 1	Model 2	Model 3	Model 4
Variable 1	Age	Height	Age	Age
Variable 2	Gender	Weight	Height	Height
Variable 3		BMI	Weight	Weight
Variable 4		Waist	BMI	BMI
Variable 5		Diastolic Blood Pressure	Waist	Waist
Variable 6		Systolic Blood Pressure	Diastolic Blood Pressure	Diastolic Blood Pressure
Variable 7		Pulse	Systolic Blood Pressure	Systolic Blood Pressure
Variable 8			Pulse	Pulse
Variable 9			Gender	Cholesterol
Variable 10				Triglycerides
Variable 11				Gender
Cost Model	0	0	0	0.5
AUC	0.66	0.68	0.72	0.74
Accuracy	0.595	0.63	0.6	0.67
Recall	0.08	0.35	0.51	0.52
Precision	0.334	0.60	0.60	0.62
F1 Score	0.123	0.43	0.54	0.56
Cross-Entropy	6.144	4.32	3.28	3.15
Table	[2981, 97, 1600, 122]	[2638, 440, 1137, 585]	[2486, 592, 940, 782]	[2523, 555, 900, 822]

Table 5: Performance Metrics and Model Comparison for Models 1 to 4. The table includes various clinical variables, metrics such as AUC, accuracy, recall, precision, F1 score, the cost model, cross-entropy, and the confusion matrix.

Variable	Model 5	Model 6	Model 7
Variable 1	Age	Age	Age
Variable 2	Height	Height	Height
Variable 3	Weight	Weight	Weight
Variable 4	BMI	BMI	BMI
Variable 5	Waist	Waist	Waist
Variable 6	Diastolic Blood Pressure	Diastolic Blood Pressure	Diastolic Blood Pressure
Variable 7	Systolic Blood Pressure	Systolic Blood Pressure	Systolic Blood Pressure
Variable 8	Pulse	Pulse	Pulse
Variable 9	Cholesterol	Cholesterol	Cholesterol
Variable 10	Triglycerides	Triglycerides	Triglycerides
Variable 11	Gender	Gender	Gender
Variable 12	Glycosylated Hemoglobin	Glucose	Glucose
Variable 13			Hemoglobin Glycosylated
Cost Model	4.5	2.1	6.1
AUC	0.832	0.84	0.92
Accuracy	0.739	0.766	0.81
Recall	0.526	0.612	0.739
Precision	0.774	0.777	0.786
F1 Score	0.613	0.675	0.761
Cross-Entropy	3.15	2.6	1.64
Table	[2809, 269, 838, 884]	[2784, 294, 810, 912]	[2732, 346, 492, 1230]

Table 6: Performance Metrics and Model Comparison for Models 5 to 7. The table continues with various clinical variables, metrics such as AUC, accuracy, recall, precision, F1 score, the cost model, cross-entropy, and the confusion matrix.

4.5 Uncertainty quantification

Now, we focus on applying the new uncertainty quantification algorithm proposed in Algorithm 2.3.3 based on conformal inference. To understand how uncertainty evolves according to patient characteristics, we estimate for each patient in the dataset the score function $\widehat{s}(X_1, 1)$ for a diabetes class, '1'. This is done with an additive generative model using fasting plasma glucose (FPG), heart rate, and age as predictors (see Figure 4). Particularly, the maximum uncertainty is observed in patients over 60 years old, with a higher heart rate, and when glucose levels are in the prediabetic range, $100 < \text{glucose} < 125\text{mg/dL}$. For patients older than 60 years, uncertainty decreases, as it does for normoglycemic patients or those with a clear diabetic pattern according to FPG values. Overall, young individuals with a low heart rate and low fasting glucose levels are the patients for whom the model's discrimination capacity is higher, based on young healthy individuals. In the case of prediabetic individuals, particularly elderly ones with a higher heart rate, uncertainty increases significantly, and more routine medical testing is advisable.

5 Discussion

The present article introduces a new predictive framework based on neural network models that incorporate automatic uncertainty quantification for predictive output steps across different complex sample designs, such as stratified designs, Bernoulli sampling, and maximum entropy sampling. Utilizing the theory of empirical processes, we have established the asymptotic theory, ensuring the universal consistency of the regression function as well as the asymptotic normality

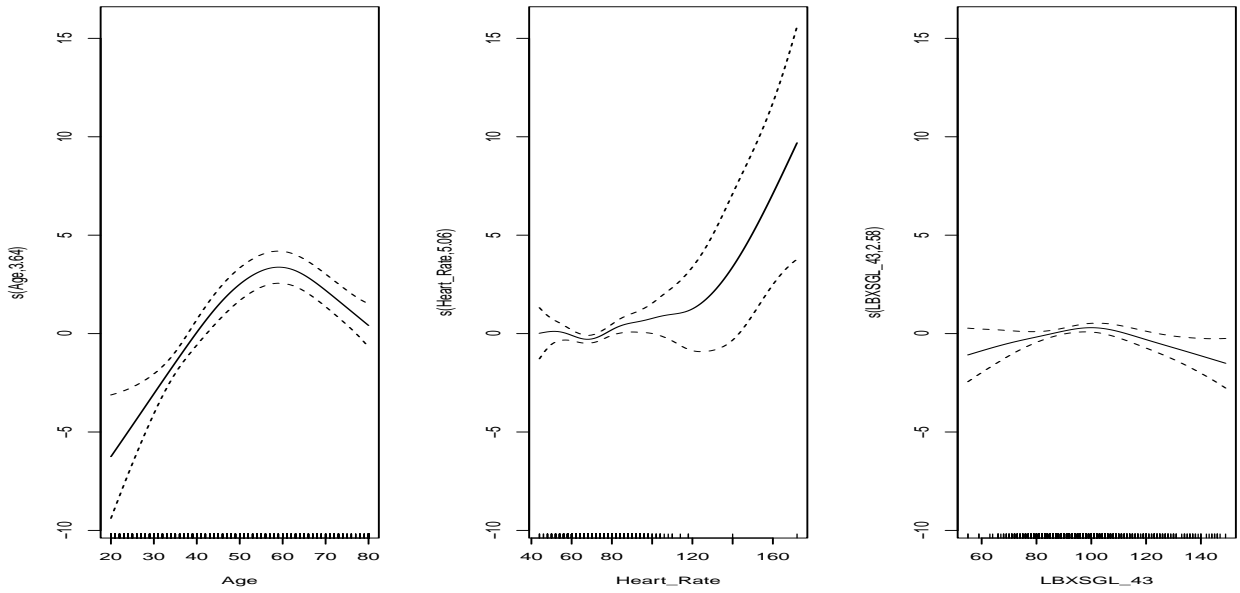


Figure 4: Covariate effect to predict the score function estimated with a new conformal survey prediction algorithm

of the neural network parameters. For the uncertainty algorithm under certain exchangeability conditions, we establish non-asymptotic guarantees, while the consistency of predictive regions is assured through the universal consistency of all regression functions.

Through various simulation scenarios in classification settings, we demonstrate the effective behavior of these methods for finite sample sizes and their consistency properties for pointwise estimation and uncertainty quantification of prediction outputs.

In specific clinical applications aimed at predicting the risk of diabetes mellitus using data from NHANES 2011-2014, we explored models of varying complexity and economic costs. From a public health perspective, the results are significant as they enable the quantification of diabetes risk with models of different complexity and healthcare resources, offering varying efficacy. Despite their simplicity, some models remain effective in different patient subgroups, aiding in the screening of diabetes risk. The uncertainty quantification analysis reveals that age, elevated heart rate, and baseline glucose values in the prediabetes range increase the uncertainty of model predictions. In terms of overall prediction capacity, even when using main diagnostic criteria, classic classification performance may not be achieved due to patients who may have normal glucose values but were previously diagnosed with diabetes. In a model not measuring lab variables, the overall AUC is 0.74, comparable to traditional diabetes scores, but considering anthropometric and heart variables in conjunction with basic patient characteristics. Recently, a commentary in a paper published in Nature Digital Medicine journal [26] emphasized the inconsistency of diabetes score results due to the observational nature of the cohorts and limited experimental design, a reason we highlighted in the introduction regarding the reproducibility crisis. Our models offer population reproducibility. Future data analysis steps include creating phenotypes of patients in terms of uncertainty or analyzing with interpretable clinical rules subphenotypes of patients where the model’s discriminative capacity is high, for example, AUC-dependent ROC analysis. For patients with large uncertainty or low prediction capacity, this can be crucial in establishing personalized follow-ups, finding alternative measurement strategies, or incorporating longitudinal information into the models.

From a methodological standpoint, despite the extensive literature on classical regression models for surveys, the application of machine learning is rare. Here, we propose the first general methodology based on neural networks that also introduces metrics to quantify uncertainty and provide quantile predictions. The codes and analyses are available on GitHub, encouraging the adoption of models that can enhance outcomes in precision public health and traditional epidemiology through surveys. For instance, over 50,000 new clinical studies are documented in NHANES, underscoring the need to equip practitioners with reliable data analysis tools for deriving generalizable conclusions in their studies.

For future work, we suggest expanding the methods used here, such as their application to time-to-event analysis or the development of specific techniques to handle covariate functions, or creating new diagnostic tests with conditional ROC curve analysis [19] to assess prediction capabilities in survey cohorts like NHANES.

In summary, our work provides a robust and well-established predictive framework based on neural networks for survey designs, offering accessible methods publicly available on GitHub. These can be invaluable to the scientific community for analyzing their data directly and addressing specific scientific modeling questions.

References

- [1] Gary An. The crisis of reproducibility, the denominator problem and the scientific role of multi-scale modeling. *Bulletin of mathematical biology*, 80(12):3071–3080, 2018.
- [2] American Diabetes Association. 2. classification and diagnosis of diabetes: standards of medical care in diabetes, 2020. *Diabetes care*, 43(Supplement_1):S14–S31, 2020.
- [3] Christopher RS Banerji, Tapabrata Chakraborti, Chris Harbron, and Ben D MacArthur. Clinical ai tools must convey predictive uncertainty for each individual patient. *Nature medicine*, 29(12):2996–2998, 2023.
- [4] Rina Foygel Barber, Emmanuel J Candes, Aaditya Ramdas, and Ryan J Tibshirani. Conformal prediction beyond exchangeability. *arXiv preprint arXiv:2202.13415*, 2022.
- [5] C Glenn Begley and John PA Ioannidis. Reproducibility in science: improving the standard for basic and preclinical research. *Circulation research*, 116(1):116–126, 2015.
- [6] Valerie Bradley and Thomas E Nichols. Addressing selection bias in the uk biobank neurological imaging cohort. *MedRxiv*, pages 2022–01, 2022.
- [7] Avivit Cahn, Avi Shoshan, Tal Sagiv, Rachel Yesharim, Ran Goshen, Shalev Varda, and Itamar Raz. Prediction of progression from pre-diabetes to diabetes: Development and validation of a machine learning model. *Diabetes metabolism. Research and Reviews*, 36(2):e3252, 2020.
- [8] Maxime Cauchois, Suyash Gupta, and John C Duchi. Knowing what you know: valid and validated confidence sets in multiclass and multilabel prediction. *J. Mach. Learn. Res.*, 22:81–1, 2021.
- [9] Prevention CDC. National diabetes statistics report: estimates of diabetes and its burden in the united states, 2020. *Atlanta, GA: US Department of Health and Human Services*, 2020.

- [10] Björn Dahlöf. Cardiovascular disease risk factors: epidemiology and risk assessment. *The American journal of cardiology*, 105(1):3A–9A, 2010.
- [11] Jianqing Fan, Cong Ma, and Yiqiao Zhong. A selective overview of deep learning. *Statistical science: a review journal of the Institute of Mathematical Statistics*, 36(2):264, 2021.
- [12] Raphael A Fraser, Stuart R Lipsitz, Debajyoti Sinha, and Garrett M Fitzmaurice. A note on median regression for complex surveys. *Biostatistics*, 23(4):1074–1082, 10 2021.
- [13] Ziad Akram Ali Hammouri, Pablo Rodríguez Mier, Paulo Félix, Mohammad Ali Mansournia, Fernando Huelin, Martí Casals, and Marcos Matabuena. Uncertainty quantification in medicine science: The next big step. *Archivos de bronconeumologia*, 59(11):760–761, 2023.
- [14] Qiyang Han and Jon A. Wellner. Complex sampling designs: Uniform limit theorems and applications. *The Annals of Statistics*, 49(1):459 – 485, 2021.
- [15] Torsten Harms and Pierre Duchesne. On kernel nonparametric regression designed for complex survey data. *Metrika*, 72:111–138, 2010.
- [16] Geronimo Heilmann, Sandra Trenkamp, Clara Möser, Maria Bombrich, Martin Schön, Iryna Yurchenko, Klaus Strassburger, Marcos Matabuena Rodríguez, Oana-Patricia Zaharia, Volker Burkart, et al. Precise glucose measurement in sodium fluoride-citrate plasma affects estimates of prevalence in diabetes and prediabetes. *Clinical Chemistry and Laboratory Medicine (CCLM)*, (0), 2023.
- [17] Klaus Hoeyer. Data as promise: Reconfiguring danish public health through personalized medicine. *Social studies of science*, 49(4):531–555, 2019.
- [18] Daniel G Horvitz and Donovan J Thompson. A generalization of sampling without replacement from a finite universe. *Journal of the American statistical Association*, 47(260):663–685, 1952.
- [19] Holly Janes and Margaret S Pepe. Adjusting for covariate effects on classification accuracy using the covariate-adjusted roc curve. 2006.
- [20] Clifford Leroy Johnson, Sylvia M Dohrmann, Vicki L Burt, and Leyla Kheradmand Mohadjer. *National health and nutrition examination survey: sample design, 2011-2014*. Number 2014. US Department of Health and Human Services, Centers for Disease Control and Prevention, 2014.
- [21] Thomas Lumley and Alastair Scott. Fitting regression models to survey data. *Statistical Science*, pages 265–278, 2017.
- [22] K Makrilakis, S Liatis, S Grammatikou, D Perrea, C Stathi, P Tsiligros, and N Katsilambros. Validation of the finnish diabetes risk score (findrisc) questionnaire for screening for undiagnosed type 2 diabetes, dysglycaemia and the metabolic syndrome in greece. *Diabetes & metabolism*, 37(2):144–151, 2011.
- [23] Laurie T Martin, Teague Ruder, José J Escarce, Bonnie Ghosh-Dastidar, Daniel Sherman, Marc Elliott, Chloe E Bird, Allen Fremont, Charles Gasper, Arthur Culbert, et al. Developing predictive models of health literacy. *Journal of general internal medicine*, 24:1211–1216, 2009.

- [24] Marcos Matabuena, Paulo Félix, Ziad Akram Ali Hammouri, Jorge Mota, and Borja del Pozo Cruz. Physical activity phenotypes and mortality in older adults: a novel distributional data analysis of accelerometry in the nhanes. *Aging Clinical and Experimental Research*, 34(12):3107–3114, 2022.
- [25] Marcos Matabuena and Alexander Petersen. Distributional data analysis of accelerometer data from the nhanes database using nonparametric survey regression models. *Journal of the Royal Statistical Society Series C: Applied Statistics*, 72(2):294–313, 2023.
- [26] Farida Mohsen, Hamada RH Al-Absi, Noha A Yousri, Nady El Hajj, and Zubair Shah. A scoping review of artificial intelligence-based methods for diabetes risk prediction. *npj Digital Medicine*, 6(1):197, 2023.
- [27] Kristin Mühlenbruch, Rebecca Paprott, Hans-Georg Joost, Heiner Boeing, Christin Heidemann, and Matthias B Schulze. Derivation and external validation of a clinical version of the german diabetes risk score (gdrs) including measures of hba1c. *BMJ Open Diabetes Research and Care*, 6(1):e000524, 2018.
- [28] Marcus R Munafò, Chris Chambers, Alexandra Collins, Laura Fortunato, and Malcolm Macleod. The reproducibility debate is an opportunity, not a crisis. *BMC Research Notes*, 15(1):43, 2022.
- [29] Emily D Parker, Janice Lin, Troy Mahoney, Nwanneamaka Ume, Grace Yang, Robert A Gabbay, Nuha A ElSayed, and Raveendhara R Bannuru. Economic costs of diabetes in the us in 2022. *Diabetes Care*, 47(1):26–43, 2024.
- [30] David S Robertson, Kim May Lee, Boryana C López-Kolkovska, and Sofía S Villar. Response-adaptive randomization in clinical trials: from myths to practical considerations. *Statistical science: a review journal of the Institute of Mathematical Statistics*, 38(2):185, 2023.
- [31] James M Swanson. The uk biobank and selection bias. *The Lancet*, 380(9837):110, 2012.
- [32] Clare Turnbull, Helen V Firth, Andrew OM Wilkie, William Newman, F Lucy Raymond, Ian Tomlinson, Robin Lachmann, Caroline F Wright, Sarah Wordsworth, Angela George, et al. Population screening requires robust evidence,Äigenomics is no exception. *The Lancet*, 403(10426):583–586, 2024.
- [33] Vladimir Vovk, Alexander Gammerman, and Glenn Shafer. *Algorithmic learning in a random world*, volume 29. Springer, 2005.
- [34] Timothy L Wiemken and Robert R Kelley. Machine learning in epidemiology and health outcomes research. *Annu Rev Public Health*, 41(1):21–36, 2020.
- [35] Yang Wu, Haofei Hu, Jinlin Cai, Runtian Chen, Xin Zuo, Heng Cheng, and Dewen Yan. Machine learning for predicting the 3-year risk of incident diabetes in chinese adults. *Frontiers in Public Health*, 9, 2021.
- [36] Frank Yates. Sir ronald fisher and the design of experiments. *Biometrics*, 20(2):307–321, 1964.